Synthesis, Spectroscopic and Structural Characterization of Mono- and Bi-nuclear Iron(II) Complexes with 2,6-Diacetylpyridine Bis(acylhydrazones)†

Alex Bonardi, Clara Carini, Curzio Merlo, Corrado Pelizzi,* Giancarlo Pelizzi, Pieralberto Tarasconi, and Francesca Vitali
Istituto di Chimica Generale, Centro di Studio per la Strutturistica Diffrattometrica del C.N.R., Viale delle Scienze, 43100 Parma, Italy
Fabrizio Cavatorta
Dipartimento di Fisica, Viale delle Scienze, 43100 Parma, Italy

The synthesis and the i.r., u.v.–visible, and ^{57}Fe Mössbauer spectroscopic characterization of a series of mono- and bi-nuclear (homo and hetero) iron(II) complexes with three bis(acylhydrazones) (acyl = 2-pyridinecarbonyl, salicyloyl, or 2-thenoyl) and the mono(2-thenoylhydrazone) of 2,6-diacetylpyridine are given and discussed. The *X*-ray structure analysis of dichloro-[2,6-diacetylpyridine bis(salicyloylhydrazone)]iron(II)-water-toluene (1/1/0.5) has been performed.

As a part of a research program mainly directed to the synthesis of more flexible and versatile ligands, we have investigated the chelating properties of 2,6-diacetylpyridine acylhydrazones in metal complexes. This study revealed a variety of different conformations and/or configurations.[1–3] It has been now extended to homo- and hetero-binuclear metal complexes,[4] in order to produce bi- or poly-metallic species, which are of interest in connection with spin exchange and charge transfer between metal ions and with their use as catalysts or promoters of organic syntheses.[5–10]

In this paper we describe the synthesis, i.r., u.v.–visible, and ^{57}Fe Mössbauer spectroscopic characterization of a series of mono- and bi-nuclear (homo and hetero) iron(II) complexes with the following acylhydrazones: 2,6-diacetylpyridine mono-(2-thenoylhydrazone) (Hdapmt), 2,6-diacetylpyridine bis(2-pyridinecarbonylhydrazone) (H_2dappc), 2,6-diacetylpyridine bis(salicyloylhydrazone) (H_2daps), and 2,6-diacetylpyridine bis(2-thenoylhydrazone) (H_2dapt). The *X*-ray crystal structure of the complex $[Fe(H_2daps)Cl_2]\cdot H_2O\cdot 0.5C_6H_5Me$ is also reported.

Experimental

Preparations.—Organic solvents were purified using published procedures.[11] Solvents were thoroughly deoxygenated beforehand and reaction mixtures were refluxed under a stream of nitrogen. Iron(II) acetate and chloride were commercially available (Aldrich). 2,6-Diacetylpyridine bis(2-pyridinecarbonylhydrazone) (H_2dappc), bis(salicyloylhydrazone) (H_2daps), and bis(2-thenoylhydrazone) (H_2dapt) were prepared by treating 2,6-diacetylpyridine with the appropriate hydrazide, as described.[12–14] All samples were prepared using Fe in natural isotopic composition.

2,6-*Diacetylpyridine mono*(2-*thenoylhydrazone*) (Hdapmt). The compound was obtained by adding dropwise an ethanol solution of thiophene-2-carbohydrazide to a hot ethanol solution of 2,6-diacetylpyridine (1:1 molar ratio). The solution was refluxed for *ca.* 2 h. A pale yellow microcrystalline product (m.p. 228—229 °C) was isolated on cooling and standing overnight [*m*/*z* = 287 (1.9), 252 (1.9), 235 (1.0), 176 (52.4), 148 (57.3), 130 (32.0), 111 (100.0), and 83 (15.5%)]. The mass spectrum revealed the presence of two conformational *E* and *Z* isomers in comparable yields; the lower volatility of the *Z* isomer is in agreement with the presence of intermolecular hydrogen bonds.

Homonuclear iron complexes. All the complexes were obtained by adding powdered anhydrous iron(II) chloride (or acetate) to an ethanol solution of the hydrazone (1:1 molar ratio). The solution was then refluxed for *ca.* 2 h and allowed to stand overnight. In all cases the final product was isolated in high yield (90—95%) by filtration under a nitrogen atmosphere. Almost all the compounds were isolated as hydrated products. In the reaction of H_2dappc with iron(II) chloride two different compounds were obtained according to whether an excess or a deficiency of the ligand was employed.

Heteronuclear iron complexes. Anhydrous $FeCl_2$, $MCl_2\cdot nH_2O$ (M = Cu, *n* = 2; M = Mn, *n* = 4), and the hydrazone in 1:1:1 molar ratio were dissolved in absolute ethanol and refluxed for about 2 h. After slow evaporation of the solvent in all cases a microcrystalline product was isolated in high yield.

The iron/manganese complexes can be obtained also by treating the preformed iron hydrazone complex with powdered manganese at reflux in ethanol suspension while the iron/copper complexes can be isolated by the reaction of the mononuclear iron hydrazone complex with copper(II) chloride in 1:1 molar ratio following the above-mentioned experimental conditions.

Template reactions. A mixture of 2,6-diacetylpyridine, acylhydrazide, and iron(II) chloride (1:2:1 molar ratio) suspended in absolute ethanol was refluxed for 2 h. In all cases the iron complex was obtained, on cooling.

The complex $[Fe(H_2dapt)Cl_2]\cdot 2H_2O$ was isolated by using a third alternative method, which involves the reaction of the preformed $[Fe(Hdapmt)Cl_2]\cdot 0.5H_2O$ with the stoicheiometric amount of thiophene-2-carbohydrazide (1:1 molar ratio) in absolute ethanol.

Measurements.—Elemental analyses for C, H, N, and S were performed on Perkin-Elmer 240 automatic equipment. Determination of metal was by atomic absorption spectroscopy on a Perkin-Elmer 303-HGA 70 instrument. Mass spectra were recorded with a Varian CH-5 spectrometer at 70 eV (*ca.* 1.12×10^{-17} J). Conductance measurements (Table 1) in nitrobenzene at *ca.* 10^{-3} mol dm^{-3} were made on a type CDM 38 Radiometer Copenhagen conductivity bridge. Magnetic measurements at room temperature were made on a standard Gouy balance calibrated with $[Ni(en)_3][S_2O_3]$;

† *Supplementary data available:* see Instructions for Authors, *J. Chem. Soc., Dalton Trans.*, 1990, Issue 1, pp. xix—xxii.

(en = ethylenediamine); diamagnetic corrections were applied using Pascal's constants.[15] Infrared spectra (4 000—200 cm^{-1}) of KBr discs were recorded on a Perkin-Elmer 283 B spectrophotometer (Philips PW 9512/00 cell), electronic spectra (900—400 nm) of methanol solutions on a Jasco 505 spectrophotometer.

The ^{57}Fe absorption Mössbauer measurements were performed by using a conventional spectrometer working at constant acceleration, equipped with a 20-mCi ^{57}Co source in a rhodium matrix. Experiments were carried out at constant temperature keeping the absorbers in a cryostat at 78—300 K. All isomeric shifts are referred to metallic iron at 298 K.

X-Ray Crystallography of $[Fe(H_2daps)Cl_2]\cdot H_2O\cdot 0.5C_6H_5Me$.—The crystal selected for data collection was a well formed parallelepiped with approximate dimensions 0.34 × 0.52 × 0.94 mm. A reciprocal-lattice search revealed no systematic absences or symmetry, indicating a triclinic lattice. The choice of the centric space group $P\bar{1}$ in preference to $P1$ was based on statistical tests for the normalized structure factors and later confirmed by the successful structure analysis. Measurements were carried out at room temperature with a computer-controlled Siemens AED single-crystal diffractometer using niobium-filtered molybdenum radiation (λ = 0.710 69 Å).

Crystal data. $C_{26.5}H_{27}Cl_2FeN_5O_5$, M = 622.29, triclinic, space group $P\bar{1}$, a = 10.281(2), b = 10.729(5), c = 14.749(5) Å, α = 82.94(2), β = 83.80(3), γ = 60.86(2)°,* U = 1 408.0(9) $Å^3$, Z = 2, D_c = 1.468 g cm^{-3}, μ(Mo-K_α) = 7.69 cm^{-1}, F(000) = 642.

Unit-cell constants, with estimated standard deviations, were determined by a least-squares fit of 28 diffractometer-measured reflections chosen in diverse regions of reciprocal space. A total of 4 234 reflections were measured with the use of the θ—2θ step-scanning mode in the range $6.0 < 2\theta < 48.0°$ ($\pm h \pm k + l$) and the 3 088 reflections with $I > 2\sigma(I)$ were retained for structure analysis. No loss of intensity of standard reflections was detected during the data collecton. A diffraction-profile analysis was performed on all reflections using the Lehmann and Larsen algorithm.[16] The intensities were converted into relative structure amplitudes after correction for Lorentz and polarization effects. Corrections for absorption and extinction were also made using the empirical method of Walker and Stuart.[17]

The structure was solved with use of a three-dimensional Patterson map to locate the iron atom while a combination of structure-factor calculations and Fourier-difference syntheses revealed the positions of all remaining non-hydrogen atoms of the complex molecule as well as of a water molecule of solvation. Refinement was performed by full-matrix least-squares procedures based on F, minimizing the function $\Sigma w(F_o - F_c)^2$. Unit weights were used initially, while in the last stages of refinement a scheme of the form $w = 1.600/[\sigma^2(F_o) + 0.0014|F_o|^2]$ was applied. A difference map calculated after isotropic refinement indicated a region of diffuse electron density which was interpreted as a half molecule of toluene of solvation disordered over two sites about a centre of symmetry. The best resolution of this molecule had three C of occupancy 0.5 and eight C of occupancy 0.25. The same difference map indicated that also one of the hydroxyl oxygens, namely O(3), suffered from a little disorder with the more populated site having an occupancy of about 0.8. The height of the alternative component, located at the other *ortho* position, was considered too low for modelling. Anisotropic parameters were assigned to all atoms except those of the two solvent molecules which were refined isotropically. The hydrogen positions of the hydrazone moiety were located by Fourier difference techniques or calculated with the exception of those of the hydroxyl groups. Refinement converged to R 0.0668 and R' 0.0884 with a goodness of fit of 2.2975. No chemically significant peaks were present in the final difference map. Atomic scattering factors used in all calculations take into account the anomalous scattering effects as in ref. 18.

Program packages used were SHELX 76[19] for solution and refinement, PARST[20] for molecular geometry calculations, and ORTEP[21] for drawing. Computations were performed on GOULD 32/77 and 6040 computers. Final atomic parameters of non-hydrogen atoms with their standard deviations are listed in Table 2, important bond distances and angles in Table 3.

Additional material available from the Cambridge Crystallographic Data Centre comprises H-atom co-ordinates, thermal parameters, and remaining bond distances and angles.

* A conventional triclinic cell with dimensions a = 10.281, b = 10.648, c = 14.749 Å, α = 91.12, β = 96.20, and γ = 118.35° can be obtained by applying the matrix −100,1 − 10,001.

Results and Discussion

As expected on the basis of previous results for a series of copper complexes of formula $Cu_2(dappc)X_2$ (X = Cl, NO_3 or ClO_4),[22,23] 2,6-diacetylpyridine bis(acylhydrazones) can form bimetallic complexes, the nature of which can be either homo- or hetero-nuclear as in the iron(II) complexes $[FeMLCl_2]$ [M = Fe, Mn, or Cu; L = 2,6-diacetylpyridine bis(acylhydrazonate)].

With the exception of the complex obtained from the reaction of iron(II) acetate, all the mononuclear complexes contain the hydrazone in its neutral form, while in the dinuclear complexes the ligand is always doubly deprotonated. All the isolated complexes are stable in air in the solid state, while a slow oxidation was observed in alcoholic solution. Methanol, ethanol, and dimethyl sulphoxide are good solvents in almost all cases, whereas there is only slight solubility in acetonitrile and tetrahydrofuran.

The heterobimetallic complexes can be isolated by using different methodologies, which also include template reactions, in agreement with the strong chelating properties of the 2,6-diacetylpyridine bis(acylhydrazones) and with the high stability of this kind of complexes.

Owing to the poor solubility, conductivity measurements were carried out only on a limited number of samples, all of which revealed a non-electrolyte nature,[24] in agreement with co-ordination of the chlorine atoms.

The magnetic susceptibility determined for some mono- and bi-metallic complexes revealed in all cases a high-spin nature (Table 1). A magnetic moment slightly slower than the spin-only value was observed for the complex $[Fe_2(dappc)Cl_2]\cdot H_2O$, in agreement with a dinuclear structure with a very weak spin–spin coupling. The magnetic susceptibility in the range from −180 to 30 °C was determined for the latter compound in order to verify the influence of the temperature on the magnetic moment (Table 4).

X-Ray Structure of $[Fe(H_2daps)Cl_2]\cdot H_2O\cdot 0.5C_6H_5Me$.—The crystal structure consists of $Fe(H_2daps)Cl_2$ units and solvating water and toluene molecules. Figure 1 presents a perspective view of the complex molecule with the atom numbering scheme and the thermal ellipsoids. The iron atom exhibits a pentagonal-bipyramidal co-ordination geometry with the equatorial plane defined by the N_3O_2 donor set of the hydrazone ligand and the two chlorine atoms in the axial positions. The five equatorial atoms are co-planar within experimental error, and the iron atom is slightly displaced (0.06 Å) toward Cl(1).

Due to geometric requirements of H_2daps, the O(1)–Fe–O(2) angle is 78.5(2)° and represents the largest deviation from a

Table 1. Physical and analytical data[a]

Complex[b]	Colour	Analysis/% C	H	N	Fe	Mn or Cu
$[Fe(Hdapmt)Cl_2]\cdot 0.5H_2O$	Green	40.2 (39.8)	3.5 (3.3)	10.1 (9.9)	12.9 (13.2)	—
$[Fe(H_2dapt)Cl_2]\cdot 2H_2O$	Green	40.1 (39.7)	4.0 (3.7)	11.9 (12.2)	10.2 (9.7)	—
$[Fe(dapt)]\cdot 2H_2O$	Brown	45.8 (45.5)	4.0 (3.8)	14.1 (14.0)	10.8 (11.1)	—
$[FeCu(dapt)Cl_2]\cdot 0.5H_2O$[c]	Brown	37.4 (37.5)	3.0 (2.7)	11.9 (11.5)	9.9 (9.2)	11.1 (10.4)
$[FeMn(dapt)Cl_2]\cdot H_2O$[c]	Red	37.8 (37.5)	3.1 (2.8)	11.2 (11.5)	9.8 (9.2)	8.7 (9.0)
$[Fe(H_2daps)Cl_2]\cdot H_2O\cdot 0.5C_6H_5Me$[c]	Green	51.5 (51.1)	4.5 (4.1)	11.2 (11.3)	9.4 (9.0)	—
$[Fe(H_2daps)Cl_2]\cdot H_2O$	Green	48.3 (47.9)	4.2 (4.0)	11.9 (12.2)	10.0 (9.7)	—
$[FeMn(daps)Cl_2]$[c]	Red	45.4 (45.2)	3.4 (3.1)	11.2 (11.5)	9.8 (9.1)	8.4 (8.9)
$[Fe(H_2dappc)Cl_2]\cdot 2H_2O$[c]	Green	45.1 (44.7)	4.2 (4.1)	17.0 (17.4)	11.1 (10.4)	—
$[Fe_2(dappc)Cl_2]\cdot H_2O$	Brown	41.9 (42.0)	3.5 (3.2)	16.0 (16.3)	18.2 (18.6)	—
$[FeCu(dappc)Cl_2]\cdot H_2O$	Brown	41.8 (41.5)	3.3 (3.2)	16.2 (16.1)	8.8 (9.2)	9.9 (10.5)
$[FeMn(dappc)Cl_2]\cdot 4H_2O$	Red	38.9 (38.6)	4.0 (3.9)	14.8 (15.0)	9.1 (8.6)	7.9 (8.4)

[a] Calculated values are given in parentheses. [b] Sulphur analysis: $[Fe(Hdapmt)Cl_2]\cdot 0.5H_2O$, 7.4 (7.6); $[Fe(H_2dapt)Cl_2]\cdot 2H_2O$, 11.2 (11.2); $[Fe(dapt)]\cdot 2H_2O$, 13.0 (12.8); $[FeCu(dapt)Cl_2]\cdot 0.5H_2O$, 10.9 (10.5); $[FeMn(dapt)Cl_2]\cdot H_2O$, 10.3 (10.5%). Magnetic moments: $[FeCu(dapt)Cl_2]\cdot 0.5H_2O$, $\mu_{Fe} = 5.09$, $\mu_{Cu} = 2.55$; $[Fe(H_2daps)Cl_2]\cdot H_2O\cdot 0.5C_6H_5Me$, $\mu = 5.17$. $[FeCu(dappc)Cl_2]\cdot H_2O$, $\mu_{Fe} = 4.70$, $\mu_{Cu} = 2.35$; $[FeMn(dappc)Cl_2]\cdot 4H_2O$, $\mu_{Fe} = 4.73$, $\mu_{Mn} = 5.29$ B.M. (B.M. $\approx 9.27 \times 10^{-24}$ J T^{-1}). [c] Non-electrolyte.

Table 2. Fractional atomic co-ordinates ($\times 10^5$ for Fe, $\times 10^4$ for Cl, O, N, and C) for $[Fe(H_2daps)Cl_2]\cdot H_2O\cdot 0.5C_6H_5Me$

Atom	*X/a*	*Y/b*	*Z/c*	Atom	*X/a*	*Y/b*	*Z/c*
Fe	23 848(10)	31 219(9)	22 768(6)	C(6)	3 587(7)	−886(7)	1 302(4)
Cl(1)	4 725(2)	2 895(2)	2 201(1)	C(7)	3 170(7)	583(7)	1 417(4)
Cl(2)	−141(2)	3 528(2)	2 451(1)	C(8)	2 129(7)	3 790(7)	206(4)
O(1)	3 101(5)	1 003(4)	2 198(3)	C(9)	2 257(7)	3 543(7)	−773(4)
O(2)	2 615(5)	2 338(4)	3 691(3)	C(10)	1 595(7)	5 217(6)	530(4)
O(3)	3 339(7)	−495(6)	−344(4)	C(11)	1 095(7)	6 485(7)	−9(4)
O(4)	1 526(6)	4 931(5)	5 802(3)	C(12)	567(8)	7 726(7)	385(5)
O(5)	−1 365(16)	1 089(12)	1 844(8)	C(13)	537(8)	7 723(7)	1 327(5)
N(1)	2 869(6)	1 450(5)	655(3)	C(14)	1 072(7)	6 428(6)	1 830(4)
N(2)	2 432(6)	2 831(6)	849(3)	C(15)	1 160(7)	6 246(6)	2 845(4)
N(3)	1 563(5)	5 201(5)	1 456(3)	C(16)	769(9)	7 463(7)	3 396(5)
N(4)	1 650(6)	4 943(5)	3 151(3)	C(17)	2 348(7)	3 140(6)	4 293(4)
N(5)	1 834(6)	4 561(5)	4 063(3)	C(18)	2 582(7)	2 626(7)	5 266(4)
C(1)	3 888(8)	−1 867(7)	2 068(5)	C(19)	3 248(8)	1 151(7)	5 458(4)
C(2)	4 285(8)	−3 279(7)	1 975(6)	C(20)	3 575(9)	540(8)	6 349(5)
C(3)	4 394(9)	−3 729(9)	1 113(6)	C(21)	3 157(9)	1 435(9)	7 041(4)
C(4)	4 124(8)	−2 804(8)	354(5)	C(22)	2 509(8)	2 869(8)	6 875(4)
C(5)	3 695(7)	−1 381(8)	424(5)	C(23)	2 204(7)	3 479(7)	5 980(4)

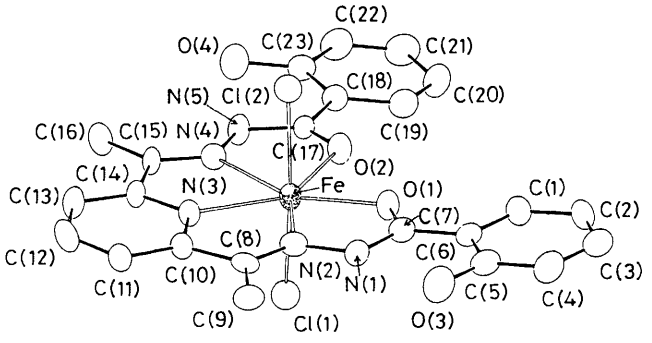

Figure 1. ORTEP drawing of the structure of $[Fe(H_2daps)Cl_2]\cdot H_2O\cdot 0.5C_6H_5Me$

regular pentagonal-bipyramidal geometry where it would be 72°. The other angles subtended at iron by pairs of atoms in the girdle range from 67.9(2) to 73.5(2)°. The angle between the apical ligands is 174.7(1)° and those between apical and equatorial atoms are close to 90° [range 87.2(2)—95.2(2)°]. By virtue of the chelating action of H_2daps there are four five-membered chelate rings in the structure, all of which are almost planar (no atom deviates by more than 0.04 Å from the respective least-squares plane) and slightly twisted (0.8—2.6°) out of the N_3O_2 donor plane. The two FeNCCN rings are at an angle of 2.7° to each other and inclined *ca.* 2° to the plane of the respective adjacent FeOCNN ring.

Among the structures of seven-co-ordinate iron complexes retrieved from the Cambridge Crystallographic Database Files, only one iron(III) derivative, namely dichloro[2,6-diacetylpyridine bis(semicarbazone)]iron chloride dihydrate,[25] has the same donor atoms (two Cl, two O, and three N) and so is well fit for a comparison with the present one. In spite of the different oxidation state, the two compounds are similar with respect to (*i*) the pentagonal-bipyramidal metal environment, (*ii*) the presence of two chlorines in the apical positions, (*iii*) the pentadentate ligand behaviour of the organic molecule which occupies the equatorial plane, thus giving rise to four five-membered chelate rings, and (*iv*) the values of most structural parameters in the co-ordination sphere. As regards the bond distances, the Fe–N and Fe–O distances average 2.200 and 2.102 Å, respectively, in the semicarbazone derivative and 2.204 and 2.088 Å in our compound. Worthy of comment are the

Table 3. Selected bond distances (Å) and angles (°)

Fe–Cl(1)	2.290(3)	C(5)–O(3)	1.344(9)
Fe–Cl(2)	2.404(2)	N(1)–N(2)	1.381(8)
Fe–O(1)	2.032(5)	N(2)–C(8)	1.252(8)
Fe–O(2)	2.144(4)	C(8)–C(10)	1.476(10)
Fe–N(2)	2.158(5)	C(15)–N(4)	1.272(8)
Fe–N(3)	2.210(5)	N(4)–N(5)	1.362(7)
Fe–N(4)	2.244(6)	N(5)–C(17)	1.359(8)
O(1)–C(7)	1.270(8)	O(2)–C(17)	1.228(8)
N(1)–C(7)	1.327(8)	C(17)–C(18)	1.474(8)
C(6)–C(7)	1.446(10)	C(23)–O(4)	1.365(8)
Cl(1)–Fe–Cl(2)	174.7(1)	N(2)–C(8)–C(10)	112.5(5)
O(1)–Fe–N(2)	73.5(2)	C(8)–C(10)–N(3)	113.4(5)
N(2)–Fe–N(3)	69.7(2)	C(10)–N(3)–Fe	118.5(4)
N(3)–Fe–N(4)	67.9(2)	C(14)–N(3)–Fe	122.5(4)
N(4)–Fe–O(2)	70.1(2)	C(14)–C(15)–N(4)	111.8(5)
O(2)–Fe–O(1)	78.5(2)	C(15)–N(4)–Fe	124.5(4)
Fe–O(1)–C(7)	117.8(4)	C(15)–N(4)–N(5)	120.4(5)
O(1)–C(7)–N(1)	122.8(6)	N(5)–N(4)–Fe	115.0(4)
C(7)–N(1)–N(2)	110.5(5)	N(4)–N(5)–C(17)	114.0(5)
N(1)–N(2)–Fe	115.2(4)	N(5)–C(17)–O(2)	119.4(5)
N(1)–N(2)–C(8)	119.2(5)	C(17)–O(2)–Fe	121.3(4)
C(8)–N(2)–Fe	125.5(5)		

Table 4. Magnetic properties of $[Fe_2(dappc)Cl_2]\cdot H_2O$

T/K	$10^6\chi'_M$/cm^3 mol^{-1}	μ/B.M.
93	23 930.55	4.24 (3.00)
123	23 617.45	4.84 (3.42)
153	22 193.84	5.23 (3.70)
183	21 808.19	5.67 (4.01)
213	19 807.20	5.83 (4.12)
243	18 349.11	6.00 (4.24)
273	16 770.09	6.08 (4.30)
303	15 463.45	6.15 (4.35)

The values given in parentheses are referred to a single iron atom.

Fe–Cl bonds which are only slightly different in the semicarbazone derivative, 2.325(2) and 2.362(2) Å, and of unequal length in the present compound, 2.290(3) and 2.404(2) Å. A reasonable explanation is that the bond Fe–Cl(2) is weakened relative to Fe–Cl(1) because there is a hydrogen bond to Cl(2) (see below) but not to Cl(1).

Up to now, *X*-ray structures of three other metal complexes of H_2daps have been investigated in our laboratories, namely $SnPr^n_2(daps)$,[13] $[Ni(H_2daps)(OH_2)_2][NO_3]_2\cdot 1.5H_2O$,[26] and $[Cd(H_2daps)Cl_2]\cdot CHCl_3\cdot MeOH$.[27] The present investigation emphasizes the tendency of this type of ligand to favour a seven-co-ordinate pentagonal-bipyramidal geometry functioning as a N_3O_2 donor in the pentagonal girdle, thus leaving the axial positions available for two other ligands, usually water molecules, inorganic anions, or σ-bonded organic groups. The main difference among the four structures concerns the deprotonation of the hydrazone ligand which only occurs in the tin compound. It can also be added that in the nickel complex H_2daps is unsymmetrically bound to the metal, this being associated with the disparity of the two Ni–O bonds which differ by a significant 0.38 Å.

The complex molecule contains two intramolecular hydrogen bonds which occur between the hydrazidic nitrogens and the hydroxyl oxygens: N(1)···O(3) 2.525(9) Å, N(1)–H···O(3) 129°; N(5)···O(4) 2.606(7) Å, N(5)–H···O(4) 123°. As above mentioned, the crystal structure is also characterized by an intermolecular hydrogen bond which involves the hydroxyl oxygen O(4) and the more weakly co-ordinated chlorine atom: O(4)···Cl(2) ($\bar{x}$, $1-y$, $1-z$) 3.060(5) Å. The water molecule does not contribute to the formation of intermolecular hydrogen bonding and this justifies its large thermal motion; the shortest contact is O(5)···C(13) (x, $y-1$, z) 3.30(1) Å.

Infrared and Electronic Spectra.—Selected vibrational bands of the hydrazones in their free and co-ordinated forms are reported in Table 5. The different nature of the terminal aromatic rings in the bis(acylhydrazones) produces some vibrational differences in the frequency values of functional groups such as CO, NH, and CN.

It is worth comparing the frequency values of the ν(NH) bands in the 3 300—3 100 cm^{-1} region; Hdapmt and H_2dapt show low frequency values (3 155 and 3 160 cm^{-1} respectively), which can be justified by the presence of intramolecular hydrogen bonds. The high value of ν(NH) band (3 310 cm^{-1}) observed in the spectrum of H_2dappc is in accord with the absence of hydrogen bonds, previously shown by the *X*-ray structural analysis,[12] so indicating that the steric effects seem to influence the conformation (or configuration) of the hydrazone more than do the electronic effects. The latter are probably responsible for the formation of intra- and inter-molecular hydrogen bonds in the Hdapmt molecule, as confirmed by mass spectrometry which revealed two conformational isomers.

As regards the ligand behaviour of the hydrazone, the following points can be made. (*a*) With the exception of $[Fe(H_2dappc)Cl_2]\cdot 2H_2O$, the frequency values of ν(CO) ('amide I') are indicative of participation of the oxygen atom of both CO groups in the co-ordination; negative shifts are observed which are more pronounced when the hydrazone is present in its deprotonated form.[28–30] The spectrum of $[FeCu(dapt)Cl_2]\cdot 0.5H_2O$ shows a splitting of the amide I band, in agreement with the presence of two different metal–oxygen bonds, as previously observed for similar metal complexes.[26,31] In all the other heterometallic complexes only a broad amide I band is observed. In $[Fe(H_2dappc)Cl_2]\cdot 2H_2O$ only one CO group seems to be involved in the co-ordination.

(*b*) Positive shifts of the amide II band [δNH, ν(CN)] are observed for all the complexes of H_2dappc and H_2dapt, while for the H_2daps derivatives a negative shift is always present. This difference can be related to the inductive effect produced by the terminal aromatic substituent, which influences the C–N bond distance.

Owing to the poor solubility of the complexes, only the electronic spectra of six complexes, $[Fe(H_2daps)Cl_2]\cdot H_2O\cdot 0.5C_6H_5Me$, $[Fe(H_2dapt)Cl_2]\cdot 2H_2O$, $[Fe_2(dappc)Cl_2]\cdot{}_2H_2O$, $[FeMn(dappc)Cl_2]\cdot 4H_2O$, $[FeCu(dappc)Cl_2]\cdot H_2O$, and $[Fe(Hdapmt)Cl_2]\cdot 0.5H_2O$, were recorded in methanol solution. In the spectrum of $[Fe(H_2daps)Cl_2]\cdot H_2O\cdot 0.5C_6H_5Me$ two absorptions at 544 and 637 nm are present, which can be attributed to two spin-allowed Laporte-forbidden transitions (these are $^5E_1 \longrightarrow {}^5E_2$ and $^5E_1 \longrightarrow {}^5A_1$)[32,33] in agreement with a D_{5h} symmetry. In the spectrum of $[Fe(H_2dapt)Cl_2]\cdot 2H_2O$, in which the iron environment should be similar, an absorption at 595 nm is present, while a second band is probably masked by the strong charge-transfer absorption at 350—400 nm. In the other four complexes the attribution of the iron environment[33–35] is difficult owing to the presence of only one absorption in the range 510—580 nm.

The ^{57}Fe *Mössbauer Spectra of the Iron*(II) *Compounds.*—The measured Mössbauer spectra are reported in Figure 2. Best fits to the experimental spectra have been calculated by means of a program using a reduced-χ^2 criterion and a gradient algorithm, with the possibility to choose between different lineshapes and either peak or area intensity parameters. The experimental spectra have been fitted using a single doublet for all single iron complexes and two doublets for $[Fe_2(dappc)Cl_2]\cdot H_2O$. The results are summarized in Table 6.

Table 5. Selected vibrational bands (cm^{-1})

Compound	ν(OH)	ν(NH)	$\nu(CH)_{ar}$	$\nu(CH)_{alk}$	Amide I	Ring	Amide II	$\delta(CH)_{alk}$	δ(OH)	Amide III
Hdapmt	—	3 155m	3 040w	2 920w	1 690s 1 645vs	1 570m 1 500m	1 510m	1 420m 1 390m	—	1 310vs
$[Fe(Hdapmt)Cl_2]\cdot 0.5H_2O$	3 420w(br)	3 160w	3 070m	2 920w	1 670m 1 600vs	1 500m	1 520s	1 415s 1 380m	1 360s	1 305s
H_2dapt	—	3 160m	3 040w	2 920(sh)	1 635vs	1 565m 1 500m	1 510m	1 415vs 1 385s	—	1 290m
$[Fe(H_2dapt)Cl_2]\cdot 2H_2O$	3 400w(br)	3 150mw	3 060mw	2 920(sh)	1 610vs	1 500m	1 525s	1 410s 1 395w	1 350m	1 290s
$[Fe(dapt)]\cdot 2H_2O$	3 420w(br)	—	3 060w	2 910w	1 580m	—	1 525s	1 420ms 1 410ms	1 375vs	1 325s
$[FeCu(dapt)Cl_2]\cdot 0.5H_2O$	3 450w(br)	—	3 070m	2 900(sh)	1 585vs 1 580s	1 485m	1 525vs	1 430m 1 420s	1 380s	1 325s
$[FeMn(dapt)Cl_2]\cdot H_2O$	3 480m(br)	—	3 070m	2 960mw 2 910mw	1 580m(br)	1 475s	1 525s	1 425vs 1 405vs	1 370s	1 325s
H_2daps	3 200m(br)	3 290(sh)	3 070(sh)	2 920w	1 655vs 1 640(sh)	1 605m 1 490mw	1 555m 1 550m	1 455s	—	1 305m
$[Fe(H_2daps)Cl_2]\cdot H_2O\cdot 0.5C_6H_5Me$	3 410w(br)	3 270m	3 030w	2 910w	1 630vs 1 605vs	1 600s 1 485s	1 510ms	1 445ms	1 375m	1 295mw
$[Fe(H_2daps)Cl_2]\cdot H_2O$	—	3 240m	3 060w	2 920w	1 625vs	1 605vs 1 570ms	1 530ms	1 490ms 1 460(sh) 1 450ms	—	1 275m
$[FeMn(daps)Cl_2]$	—	—	3 060w	2 930w	1 610vs(br)	1 590vs	1 510s	1 490s 1 450s 1 425m	—	1 260m
$H_2dappc\cdot 0.5H_2O$	3 460mw	3 310m	3 050w	2 900w	1 695vs	1 590mw 1 565mw	1 510vs	1 450vs 1 435s	—	1 280m
$[Fe(H_2dappc)Cl_2]\cdot 2H_2O$	3 400m	3 315ms	3 050w	2 900vw	1 710s	1 560m	1 505vs	1 430m	1 380s	1 300m
$[Fe_2(dappc)Cl_2]\cdot H_2O$	3 410ms	—	3 050m	2 910w	1 605m	1 560ms 1 515ms	1 545s	1 440w 1 425w	1 380vs	1 300m
$[FeCu(dappc)Cl_2]\cdot H_2O$	3 440m(br)	—	3 070(sh) 3 050m	2 910w	1 595w(br)	1 560ms 1 520s	1 540s	1 435w 1 425w	1 380vs	1 285w
$[FeMn(dappc)Cl_2]\cdot 4H_2O$	3 350ms	—	3 050w	2 910(sh)	1 605w(br)	1 555w 1 500w	1 525s	1 470m 1 430w	1 380vs	1 285w

Table 6. Mössbauer data[a]

Spectrum	Compound	Model[b]	T/K	δ[c]	ΔE_Q	Γ[d]
				mm s^{-1}		
(*i*)	$[Fe(H_2dapt)Cl_2]\cdot 2H_2O$	s.s.d.	298	1.363(2)	2.241(4)	0.191(4)
(*ii*)	$[Fe(Hdapmt)Cl_2]\cdot 0.5H_2O$	s.s.d.	298	0.991(1)	2.728(2)	0.152(1)
(*iii*)	$[Fe(H_2daps)Cl_2]\cdot H_2O$	s.s.d.	298	1.172(1)	1.821(2)	0.179(1)
(*iv*)	$[Fe(H_2daps)Cl_2]\cdot H_2O\cdot 0.5C_6H_5Me$	s.s.d.	298	0.60(1)	0.82(1)	0.477(6)
(*v*)	$[Fe(H_2dappc)Cl_2]\cdot 2H_2O$	s.s.d.	298	0.483(5)	0.790(9)	0.424(5)
(*vi*)		s.s.d.	78	0.512(3)	0.717(5)	0.435(3)
(*vii*)	$[Fe(dapt)]\cdot 2H_2O$	s.a.d.	298	0.82(1)	1.01(1)	0.41(1), 0.40(2)[e,f]
(*viii*)		s.a.d.	78	0.958(6)	1.03(1)	0.381(6), 0.39(1)[e,g]
(*ix*)	$[FeCu(dappc)Cl_2]\cdot H_2O$	s.a.d.	298	0.51(1)	0.72(1)	0.44(1), 0.44(2)[e,h]
(*x*)	$[FeMn(dappc)Cl_2]\cdot 4H_2O$	s.a.d.	298	0.597(4)	0.55(1)	0.39(1), 0.40(2)[e,i]
(*xi*)	$[Fe_2(dappc)Cl_2]\cdot H_2O$	d.s.d.	298	0.503(4) 0.464(5)	0.51(1) 1.03(1)	0.25(1)[j] 0.32(1)

[a] Errors affecting the last figure reported in parentheses. [b] s.s.d. = Single symmetric doublet, s.a.d. = single asymmetric doublet (see text), and d.s.d. = double symmetric doublet (see text). [c] Relative to natural iron foil. [d] Full width at half maximum. [e] Independent component linewidths (low velocity, high velocity). [f] Percentage of the total doublet area subtended by the low-velocity component 76.1(1)%. [g] Percentage of the total doublet area subtended by the low-velocity component 69.0(1)%. [h] Percentage of the total doublet area subtended by the low-velocity component 63.2(2)%. [i] Percentage of the total doublet area subtended by the low-velocity component 59.4(2)%. [j] Percentage of the total doublet area subtended by the outer doublet 51.2(4)%.

Generally both the isomeric shifts δ and quadrupolar splitting ΔE_Q are of the magnitudes expected for high-spin iron(II). Some exceptions towards the lower ends of normal δ and ΔE_Q intervals are presented particularly by H_2dappc compounds. The complexes $[Fe(H_2dapt)Cl_2]\cdot 2H_2O$, $[Fe(Hdapmt)Cl_2]\cdot 0.5H_2O$, and $[Fe(H_2daps)Cl_2]\cdot H_2O$ exhibit spectra [Figure 2, spectra (*i*)—(*iii*)] typical for high-spin Fe^{2+}. The particularly high value of the quadrupolar splitting observed for $[Fe(Hdapmt)Cl_2]\cdot 0.5H_2O$ is connected with the peculiar ligand geometry of this compound leading to a higher anisotropy of the iron environment.

It is interesting that $[Fe(H_2daps)Cl_2]\cdot H_2O\cdot 0.5C_6H_5Me$ and $[Fe(H_2daps)Cl_2]\cdot H_2O$, compounds having a very similar composition and equal co-ordination plane, show totally different spectra [Figure 2, spectra (*iv*) and (*iii*)]. The spectrum of $[Fe(H_2daps)Cl_2]\cdot H_2O\cdot 0.5C_6H_5Me$ consists of a broad doublet

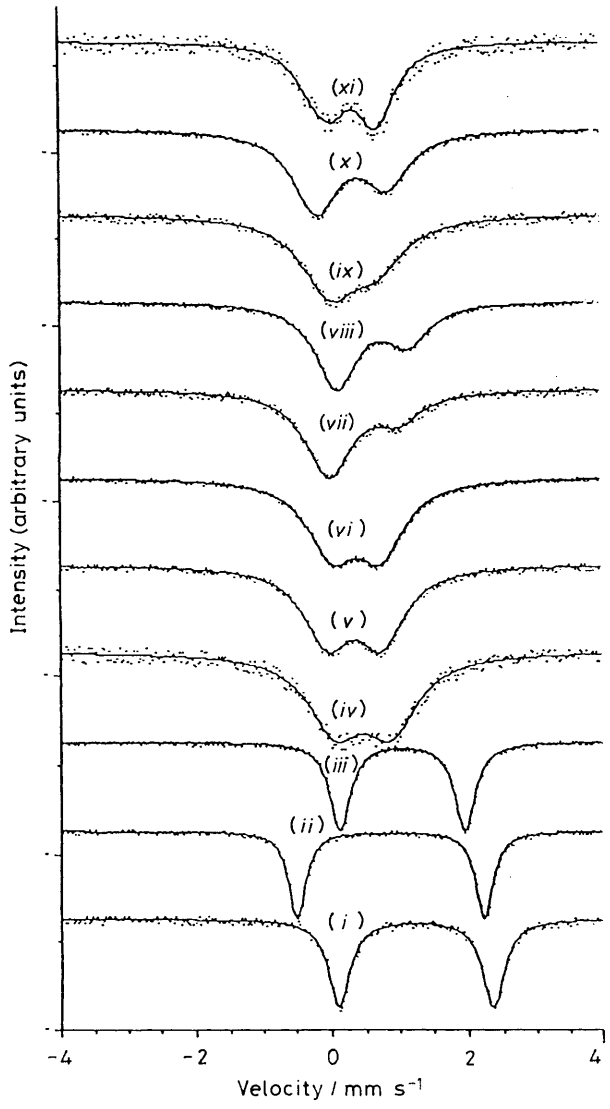

Figure 2. Mössbauer spectra together with the theoretical fitting for the complexes: $[Fe(H_2dapt)Cl_2]\cdot 2H_2O$ (*i*); $[Fe(Hdapmt)Cl_2]\cdot 0.5H_2O$ (*ii*); $[Fe(H_2daps)Cl_2]\cdot H_2O$ (*iii*); $[Fe(H_2daps)Cl_2]\cdot H_2O\cdot 0.5C_6H_5Me$ (*iv*); $[Fe(H_2dappc)Cl_2]\cdot 2H_2O$ at 298 (*v*) and 78 K (*vi*); $[Fe(dapt)]\cdot 2H_2O$ at 298 (*vii*) and 78 K (*viii*); $[FeCu(dappc)Cl_2]\cdot H_2O$ (*ix*); $[FeMn(dappc)Cl_2]\cdot 4H_2O$ (*x*); and $[Fe_2(dappc)Cl_2]\cdot H_2O$ (*xi*). All spectra at 298 K, where not stated otherwise

(Γ = 0.48 mm s^{-1}) with δ = 0.6 mm s^{-1} and ΔE_Q = 0.8 mm s^{-1}; $[Fe(H_2daps)Cl_2]\cdot H_2O$ shows a clearly defined, well separated doublet (Γ = 0.18 mm s^{-1}) with δ = 1.17 mm s^{-1} and ΔE_Q = 1.8 mm s^{-1}. Differences observed in the Mössbauer spectral parameters can be reasonably ascribed to the presence of different apical atoms and to a different packing of the molecules in the microcrystals.

The complex $[Fe(H_2dappc)Cl_2]\cdot 2H_2O$ [Figure 2, spectrum (*v*)] displays a broad doublet with Γ, δ, and ΔE_Q values similar to those measured for $[Fe(H_2daps)Cl_2]\cdot H_2O\cdot 0.5C_6H_5Me$; the spectrum of this complex does not noticeably change by lowering the temperature to 78 K [Figure 2, spectrum (*vi*)].

Although the iron atom in $[Fe(dapt)]\cdot 2H_2O$ occupies a well defined position, a marked asymmetry of the Mössbauer doublet [Figure 2; spectrum (*vii*)] was observed. The spectrum profile did not change very much when the sample temperature was lowered to 78 K [Figure 2, spectrum (*viii*)]. The complexes $[FeCu(dappc)Cl_2]\cdot H_2O$ [Figure 2, spectrum (*ix*)] and $[Fe\text{-}Mn(dappc)Cl_2]\cdot 4H_2O$ [spectrum (*x*)] display a behaviour very similar to that of $[Fe(dapt)]\cdot 2H_2O$; however, in this case, due to the presence of two possible iron binding sites, the asymmetry could also be explained in terms of a distribution of the iron atoms on the two available sites; for this reason two different fitting models have been tested, corresponding to the two possible situations: (*a*) iron distributed on the two sites (two symmetric doublets); (*b*) iron occupying a well defined site (a single doublet, evidently asymmetric). A substantially better value for χ^2 was obtained in case (*b*), thus suggesting that Fe and, as a consequence, Mn and Cu, does prefer a single site. Some specific mechanism has therefore to be invoked to explain the asymmetry of the experimental data.

Various explanations, not even mutually exclusive, can be called upon: (*i*) Goldanski–Karyagin[36,37] effect connected to the anisotropy of the recoilless fraction of the Mössbauer atom; this would be the case if, for example, very different binding constants characterized the in-plane and out-of-plane atoms; (*ii*) texture effects,[38] since the structures are markedly anisotropic, even if no spectral variation is observed when varying some detail of the sample preparation (*e.g.* grinding of the microcrystals); (*iii*) spin–spin relaxation processes, of the kind described by Blume,[39] which have been accepted as an explanation for line asymmetry for several iron complexes.[40–44] To determine uniquely which asymmetry mechanism affects the observed spectra requires many more measurements and lower temperatures and even well oriented samples.

The measured widths of the lines of the asymmetric doublets of these compounds are (Table 6) very similar, their differences being almost within the errors. As a final note on this class of spectra, asymmetry of the doublet components was observed in all the spectra of the deprotonated mononuclear complexes of iron.

Two symmetric and well separated doublets fit the spectrum of $[Fe_2(dappc)Cl_2]\cdot H_2O$ [Figure 2, spectrum (*xi*)]. The difference in the ΔE_Q values for the two doublets shows that the two iron sites have quite different local symmetry. The small δ value is explained by the low magnetic moment of this compound; almost equal areas are subtended by the two doublets which indicates that the two available sites are equally populated.

A feature common to many of the reported spectra is a certain line broadening; this is probably due to the presence of different packings of the molecules in the microcrystals leading to a small distortion of the iron surrounding with a consequent smearing of the quadrupole doublet. The low values of δ and ΔE_Q presented particularly by H_2dappc compounds can be interpreted in terms of a low average electronegativity of the iron environment; in the case of $[Fe(H_2dappc)Cl_2]$ this hypothesis is confirmed by the observation (inferred from i.r. spectra) that only one CO group is involved in the co-ordination.

Acknowledgements

The financial support of the Ministero della Pubblica Istruzione (40%) is gratefully acknowledged. We thank Mr. Andrea Cantoni for his valuable technical assistance.

References

1 M. Nardelli, C. Pelizzi, and G. Pelizzi, *Transition Met. Chem. (Weinheim, Ger.)*, 1977, **2**, 35.
2 C. Lorenzini, C. Pelizzi, G. Pelizzi, and G. Predieri, *J. Chem. Soc., Dalton Trans.*, 1983, 2155.
3 C. Pelizzi, G. Pelizzi, and P. Tarasconi, *J. Chem. Soc., Dalton Trans.*, 1985, 215.
4 A. Bonardi, C. Pelizzi, G. Pelizzi, L. Reverberi, P. Tarasconi, and F. Vitali, Congresso Interdivisionale della Societa' Chimica Italiana CISCI 89, Perugia, 1989, p. 427.

5 H. Okawa, Y. Nishida, M. Tanaka, and S. Kida, *Bull. Chem. Soc. Jpn.*, 1977, **50**, 127.
6 C. J. O'Connor, D. P. Freyberg, and E. Sinn, *Inorg. Chem.*, 1979, **18**, 1077.
7 M. G. B. Drew, J. Nelson, F. Esho, V. McKee, and S. M. Nelson, *J. Chem. Soc., Dalton Trans.*, 1982, 1837.
8 O. Kahn, J. Galy, Y. Journeaux, J. Jand, and I. Morgenstern-Badarau, *J. Am. Chem. Soc.*, 1982, **104**, 2165.
9 M. T. Yoninou, J. A. Osborn, J. P. Collin, and P. Lagrange, *Inorg. Chem.*, 1986, **25**, 453.
10 R. M. Bullock and C. P. Casey, *Acc. Chem. Res.*, 1987, **20**, 167.
11 D. D. Perrin, W. L. F. Armarego, and D. R. Perrin, 'Purification of Laboratory Chemicals,' Pergamon, Oxford, 1966.
12 C. Pelizzi and G. Pelizzi, *Acta Crystallogr., Sect. B*, 1979, **35**, 126.
13 C. Pelizzi and G. Pelizzi, *J. Chem. Soc., Dalton Trans.*, 1980, 1970.
14 C. Lorenzini, C. Pelizzi, G. Pelizzi, and G. Predieri, *J. Chem. Soc., Dalton Trans.*, 1983, 721.
15 'Modern Coordination Chemistry,' eds. J. Lewis and R. G. Wilkins, Interscience, New York, 1964.
16 M. S. Lehmann and F. K. Larsen, *Acta Crystallogr., Sect. A*, 1984, **30**, 580.
17 N. Walker and D. Stuart, *Acta Crystallogr., Sect. A*, 1983, **39**, 158.
18 'International Tables for *X*-Ray Crystallography,' Kynoch Press, Birmingham, 1974, vol. 4.
19 G. M. Sheldrick, SHELX 76, Program for Crystal Structure Determination, University of Cambridge, 1976.
20 M. Nardelli, *Comput. Chem.*, 1983, **7**, 95.
21 C. K. Johnson, ORTEP, Report ORNL-5138, Oak Ridge National Laboratory, Tennessee, 1976.
22 A. Mangia, C. Pelizzi, and G. Pelizzi, *Acta Crystallogr., Sect. B*, 1974, **30**, 2146.
23 C. Pelizzi and G. Pelizzi, unpublished work.
24 W. J. Geary, *Coord. Chem. Rev.*, 1971, **7**, 81.
25 G. J. Palenik, D. W. Wester, U. Rychlewska, and R. C. Palenik, *Inorg. Chem.*, 1976, **15**, 1814.
26 C. Pelizzi, G. Pelizzi, S. Porretta, and F. Vitali, *Acta Crystallogr., Sect. C*, 1986, **42**, 1131.
27 C. Pelizzi, G. Pelizzi, and F. Vitali, *J. Chem. Soc., Dalton Trans.*, 1987, 177.
28 K. K. Narang and A. Aggarwal, *Inorg. Chim. Acta*, 1974, **9**, 137.
29 M. F. Iskander, L. El Sayed, A. F. M. Hefny, and S. E. Zayan, *J. Inorg. Nucl. Chem.*, 1976, **38**, 2209.
30 R. L. Dutta and A. K. Sarkar, *J. Inorg. Nucl. Chem.*, 1981, **43**, 57.
31 T. J. Giorgano, G. J. Palenik, R. C. Palenik, and D. A. Sullivan, *Inorg. Chem.*, 1979, **18**, 2445.
32 M. G. B. Drew, J. Grimshaw, P. D. A. McIlroy, and S. M. Nelson, *J. Chem. Soc., Dalton Trans.*, 1976, 1388.
33 W. S. J. Kelly, G. H. Ford, and S. M. Nelson, *J. Chem. Soc. A*, 1971, 388.
34 L. J. Wilson, D. Georges, and M. A. Hoselton, *Inorg. Chem.*, 1975, **14**, 2968.
35 H. Kobayashi and Y. Yamagawa, *Bull. Chem. Soc. Jpn.*, 1972, **45**, 450.
36 V. I. Goldanskii, E. F. Makarov, and V. V. Khrapov, *Phys. Lett.*, 1963, **3**, 334.
37 S. V. Karyagin, *Dokl. Akad. Nauk SSSR*, 1963, **148**, 1102.
38 U. Gonser and H. D. Pfannes, *J. Phys. (Paris) Colloq.*, 1974, **35**, 113.
39 M. Blume, *Phys. Rev. Lett.*, 1965, **14**, 96.
40 W. M. Reiff, G. J. Long, and W. A. Baker, *J. Am. Chem. Soc.*, 1968, **90**, 6347.
41 K. S. Murray, *Coord. Chem. Rev.*, 1974, **12**, 1.
42 M. Mohan, N. S. Gupta, A. Kumar, and M. Kumar, *Inorg. Chim. Acta*, 1987, **135**, 167.
43 M. Mohan and M. Kumar, *Polyhedron*, 1985, **4**, 1929.
44 N. E. Erickson, *Adv. Chem. Ser.*, 1967, **68**.

Received 8*th December* 1989; *Paper* 9/05246A